An early signaling transcription factor regulates differentiation in *Giardia*

Han-Wei Shih, Germain C. Alas, Daria S. Rydell, Bailin Zhang, Greyson A. Hamilton, Alexander R. Paredez

Department of Biology, University of Washington, Seattle, Washington 98195

Abstract

Transcriptional regulation of differentiation is critical for parasitic pathogens to adapt to environmental changes and regulate transmission. How early signaling transcription factors (TF) activate signal transduction to initiate encystation remains an open question in *Giardia*. Here, we generate a CasRX-mediated knockdown system, together with an established CRISPRi system to screen early signaling TFs in *Giardia lamblia*. We identified an early response TF, GARP4 that regulates cyst wall protein (CWP) levels during encystation. Depletion of GARP4 increases encystation efficiency resulting in increased cyst production. Interestingly, cyst viability and CWP1 trafficking are not altered in GARP4 knockdowns, suggesting GARP4 regulates the restriction point controlling the portion of cells that terminally differentiate into cysts. Consistent with previous studies, we find that stimulation of encystation shifts the distribution of cells to the G2/M phase and these cells exhibits higher levels of CWP1, indication that entry into the encystation pathway is cell cycle regulated. Key to this increase of CWP1 in G2/M cells is activation of MYB2, a TF commonly observed during the early phase of encystation in *Giardia*. Remarkably, activated GARP4 only exhibits in G1/S cells, suggesting it has a role in preventing encystation until G2/M. Furthermore, we demonstrate that depletion of GARP4 activates MYB2 and overexpression of GARP4 represses MYB2. Our findings provide the first molecular mechanism underlying the restriction point regulating differentiation during early signaling of encystation in *Giardia lamblia*.

Introduction

To cope with environmental change, protozoa from all eukaryotic supergroups differentiate to dormant walled cysts, a process which is commonly called encystation[1]. For parasitic protozoa, deposition of cyst wall is essential to build antibiotic-resistance[2] and escape immune invasions from macrophage and neutrophils[1]. Most importantly, water-resistant cysts allow parasitic protozoa to persist in fresh water and successfully transmit infection to susceptible hosts.

Giardia is a major cause of protozoan-based diarrhea and its encystation pathway plays an important role on pathogen virulence. *Giardia* infection often occurs through consuming infectious cysts from contaminated water[3] or interpersonal contact[4], the acidic environment of the stomach activates excystation in the small intestine for colonization[5]. At the distal end of the small intestine, lipid starvation and alkaline pH trigger a portion of trophozoites to initiate

encystation[6,7]. During the early phase of *Giardia* encystation, major morphological changes occur that include cytoskeleton rearrangement, biogenesis of the Goligi-like ESVs, and cell cycle arrest[6-8].

Cell cycle arrest appears to be a common theme in encystation. Studies in *Giardia lamblia* [9], *Acanthamoeba* [10], *Entamoeba invadens* [11] have all shown that encystation stimulus causes the accumulation of G2/M cells in the early stage of encystation. In *Acanthamoeba*, encystation frequency correlates with the proportion of cells arrested at G2[10], suggesting the entry of differentiation initiates from G2/M cells. These observations led to a hypothesis that a restriction point in *Giardia*'s cell cycle also restricts encystation to cells in G2/M[9,12]. However, the molecular mechanism underlying this restriction point regulating entry into the encystation program is totally unknown.

Pioneer transcription factors (TFs), which are capable of binding condensed chromatin, possess the incredible ability to reprogram cell differentiation[13]. Several studied TFs in Giardia, such as GARP1[14], E2F1[15], WRKY[16], PAX2[17,18], ARID1[19] have been shown to be upregulated at 24 h post encystation. A recent study has shown that a MYB TF is a master regulator of differentiation in *Toxoplasma* [20]. MYB TFs also modulate encystation in *Giardia*[21] and *Entamoeba*[22]. Proteomic and RNA sequencing studies agree that MYB2 TF in *Giardia* is a key regulator in encystation[23-25]. While these observations hint that MYB2 may prompt the initiation of encystation, the upstream regulators of MYB2 are still poorly understood. Here, we screened *Giardia* transcription factors that were reported to be upregulated early in encystation based on published RNAseq data[25] for a functional role in encystation using an established CRISPRi system and a newly generated CasRX knockdown system. We identified GARP4 as an upstream regulator of MYB2 and determined that it has a key role in regulating entry into the encystation program.

Results

Characteristics of transcription factors during early encystation in *Giardia*

Given that CWP1-3 are important encystation indicators in *Giardia*[6,7,23,26,27], we first investigated CWP1-3 protein levels early in encystation using the NanoLuc expression reporter [28,29]. After exposure to encystation medium, CWP1-3 protein levels begin to increase within 1.5h and exponentially rise up at 4h (Fig 1a). To date, several TFs have been identified with roles in regulating CWP1-2, these include MYB2 [21], E2F1 [15], PAX1,2 [17,18], ARID1[19] and WRKY [16]. Whether these TFs have a role in initiating entry into the encystation pathway has not been established. This increase of CWP is likely to be signaled through early response TFs, which trigger the activation or repression of encystation specific genes. A previous transcriptomics study identified 11 TF candidates that are upregulated within 4 h of encystation [25]. We sought to test whether these TFs function as upstream regulators of encystation. Due to low confidence that some of the identified proteins were in fact transcriptional regulators, we

expressed these 11 proteins as mNeonGreen (mNG)-fusion to verify nuclear localization, using MYB2 as a positive control. MYB2 has been shown to express at 7 h in proteomic[23] and RNA sequencing studies[25] and its function of encystation has been investigated. We were able to detect nucleus localization of MYB2 at 4 h but not at 0 and 1.5 h (Fig 1b). In contrast, we observed six TFs, including MYB1, GARP4, PAX1, ARID2, E2F1 with nuclear localization at 0 h but with noticeable increases in their levels after 1.5 h of encystation stimulus (Fig 1c; Extended data 1).

We then decided to investigate the expression levels of these nucleus localized TFs. After exposure to encystation medium, GARP4 and MYB1 immediately increase within 1.5 h incubation, with GARP4 having the highest level of induction (Fig 1d). The expressions of PAX1, ARID2 and E2F1 only modestly increase at 4h (Extended data 2). That MYB1 and GARP4 are upregulated before MYB2 hints that these transcription factors may be early regulators of encystation that are upstream of MYB2 and CWP1.

Depletion of MYB2, MYB1, and GARP4 alters the encystation response

We next screened for encystation-specific TFs that are required for CWP1 synthesis, focusing on genes that were upregulated within 1.5 h of encystation. To screen for encystation specific TFs, we used an established dCas9 based CRISPRi system [26] and generated a complementary Cas13 knockdown system. Cas13 enzymes are RNA-targeting CRISPR enzymes which have been shown to have high efficiency and specificity in human cells[30]. We first expressed 3HA-tagged fusion proteins of three Cas13 enzymes (Extended data 3a), including PsCas13b[31], CasRX[30] and EsCas13d[30]. CasRX was the only Cas13 enzyme that could be expressed in *Giardia* (Extended data 3b). To establish a functional CasRX knockdown system in *Giardia lamblia*, we replaced dCas9 and gRNA scaffold sequence (SCF) with CasRX and CasRX-specific direct repeat (DR) (Extended data 3c). To determine if one of these knockdown systems might be better tolerated than the other, we examined the proportion of cells that could express dCas9 or CasRX and found no appreciable difference (Extended data 3d,e). Moreover, the growth rates were similar for cell lines that expressed CRISPRi and CasRX (Extended data 3f). To compare efficacy of knockdown, we designed CasRX- and CRISPRi-specific guide RNAs to deplete NanoLuc and CWP1, which exceeded our results with CRISPRi (Extended data 4). However, screening of gRNAs against the set of six TFs of interest revealed that efficacy varies by target gene and neither system is consistently better than the other.

As previous studies in *Giardia* have suggested that MYB2 plays a critical role in encystation[21,32], we first investigated the phenotype of CRISPRi-mediated MYB2 knockdown mutant (Fig 2a). Depletion of MYB2 reduced the CWP1 level at 4h encystation (Fig 2b,c) and totally abolished the maturation of cysts (Fig 2d), suggesting MYB2 is essential for encystation. Notably, our data is consistent with MYB2 antisense silencing mutant which reduces CWP1 expression[21]. Knockdown of MYB1 resulted in lower CWP1 and CWP2 levels (Fig 2e, Extended data 8d) as well

as fewer encysting cells (Figure 2f,g). However, the percentage of mature cysts (Figure 2h) and cyst viability (Extended data 6a) were similar to the control. This suggests that MYB1 might be an upstream regulator of CWP1 but is not essential for cyst maturation. Interestingly, depletion of GARP4 (Fig 2i) has a two-fold increase of CWP1 and an approximately 20% increase in CWP2 (Figure 2 j-k; Extended data 8d). Notably, GARP4 knockdown results in more mature cysts (Figure 2 l) without changing cyst viability (Extended data 6b). We additionally determined that knockdown of E2F1 (Extended data 5a) and PAX1 (Extended data 5d) produced less CWP1 (Extended data 5b-c, 5e-f) which agrees with published studies[15,18]. However, we unexpectedly found that, based on CWP1 expression, a higher proportion of the knockdown cell lines initiated the encystation pathway by 4h (Extended data 8a-b). Knockdown of ARID2 (Extended data 5g) did not alter CWP1 levels (Extended data 5h-i) nor change the amount of encysting cells (Extended data 8c). In summary, these results show that GARP4 is a repressor of CWP1 and cyst maturation, while MYB1 is an activator of CWP1, it is not essential for cyst maturation.

Depletion of GARP4 upregulates encystation

To further characterize the role of GARP4, we investigated whether depletion of GARP4 changes the cell growth rate and cell viability. Knockdown of GARP4 does not alter the growth rate or cell viability (Extended data 9a-b). We also observed a similar phenotype of CWP1 increase in the GARP4 mutant under two different encystation media, including two-step and lipo-protein deficient encystation media (Extended data 9c). This indicates that the GARP4 knockdown phenotype is not restricted to a specific encystation medium. Considering that GARP4 has an important role in regulating encystation, we examined how its levels change over a fine time course at the induction of encystation. Remarkably, GARP4 levels shoot up at 30 minutes while MYB1 ramps up over the first 90 minutes of encystation (Fig 3a). GARP4 mutants have consistently higher CWP1 levels during early encystation (Fig 3b). We analyzed individual cells to determine whether the increase of CWP1 in the GARP4 knockdown lines was due to increased numbers of cells entering encystation or the result of increased levels of CWP1 per cell. We collected encysting cells from different time points of encystation and stained with a CWP1 antibody to quantify encysting cells. We then investigated various phenotypes of CWP1 trafficking in GARP4 mutants. The percentage of encysting cells is 1.5-2 fold higher in GARP4 mutants at 0, 1, 2, 4, 24 h treatments (Extended data 7; Figure 3c-d). Furthermore, we analyzed CWP1-positive vesicle size and volume to address if CWP1 trafficking in the GARP4 mutant is altered. Our results show that neither vesicle size nor vesicle volume are changed (Figure 3e-f). These findings suggest that the main role of GARP4 is to modulate the portion of cells that enter the differentiation pathway.

GARP4 functions in the G1/S phase of the cell cycle

Encystation-induced G2 arrest has been demonstrated in *Giardia* [33,34]. Indeed, our data is consistent with previous studies that 1.5 h of encystation is sufficient to cause accumulation of

G2/M cells with a corresponding reduction of cells in G1/S (Figure 4a-b). To investigate whether cells in G2/M have higher CWP1, mNG-tagged CWP1 cell lines were exposed to encystation stimuli and then DNA content was measured by DRAQ5 fluorescence. We found that cells with higher DNA content had higher CWP1 levels (Extended data 10a). Similarly, G2/M cells have higher MYB2 levels, suggesting higher expression of CWP1 was due to higher level of MYB2. A prior study in *Giardia* has suggested the presence of a restriction point for entering encystation that functions to prevent cells in G1/S from initiating encystation but permits cells in G2/M to differentiate. It seemed possible that GARP4 might inhibit G1 cells from initiating encystation. We examined the relationship between GARP4::mNG and the cell cycle at 0 and 1.5 h of encystation. We found that GARP4::mNG fluorescence intensity was 1.5 fold higher in G1/S cells after exposure to encystation stimuli but slightly decreased in cells at G2/M, suggesting lower GARP4 levels permit G2/M cells to enter encystation. Because MYB2 and CWP1 levels are lower in G1 cells, we questioned if GARP4 might be an upstream repressor of MYB2. To investigate whether GARP4 is an upstream regulator of MYB2, we transfected the GARP4 CRISPRi guide RNA into MYB2-NanoLuc cell line. We found that MYB2 levels rose by 1.2 fold in the GARP4 knockdown cell line, which is consistent with MYB2 ultimately regulating CWP1 levels (Fig 4d). In contrast, overexpression of GARP4 inhibited MYB2 expression by 50% and resulted in reduced CWP1 (Fig4e). These findings suggest MYB2 is downstream of GARP4.

Since E2F1 and PAX1 have been shown to regulate CWP1-3 and MYB2, we sought to determine whether GARP4 modulates MYB2 through either E2F1 or PAX1. Interestingly, knockdowns of GARP4 does not alter E2F1 and PAX1 levels (Extended data 10b), suggesting E2F1 and PAX1 are not part of GARP4-MYB2-CWP1 pathway. Thus, MYB2 is a downstream component of GARP4 but an upstream regulator of CWP1. In this model, MYB2 is repressed in cells at G1/S by GARP4. Then during G2/M, GARP4 levels drop and MYB2 expression is triggered to induce encystation.

Discussion

In summary, we utilized CRISPRi and our newly developed CasRX-mediated knockdown tool to identify transcription factors that regulate entry into the encystation pathway. We identified GARP4, a previously unstudied TF, as a key regulator of *Giardia*'s restriction point regulating differentiation. GARP TFs are commonly considered to be plant-specific, but are also found in protists. Some plant GARP TFs are pioneering TFs for reproductive organ determination[35]. In this study, we found that GARP4 functions to prevent cells in G1/S from entering the encystation program. Our results provide the molecular mechanism for the restriction point that prevents entry into encystation until cells arrest in G2/M. We found that GARP4 depletion upregulates the formation of healthy cysts and therefore GARP4 is not required for cyst formation. Instead, GARP4 likely regulates the balance of parasite load, which most certainly has been optimized for maximal transmission. Exposure to encystation stimulus in G1/S populations triggers, GARP4 upregulation to repress CWP1 levels through inhibiting MYB2. In

contrast, GARP4 levels are slightly reduced in G2/M populations which permits activation of MYB2 to enhance CWP1 production (Fig 4). Our model explains why the frequency of G2/M cells have higher expression of CWP1.

How cells sense encystation stimulus but then induce different responses based on cell cycle status remains unknown in *Giardia*. The idea that histone deacetylase may be involved in encystation regulation is quite attractive given their function as a metabolic sensors. Only Sirutin 2.1 (GL50803_10708) is highly expressed at early phase of encystation[25]. Interestingly, Sirtuin inhibitor Nicotinamide has been shown to cause G2 arrest of cell cycle[36]. However, our data indicates that mNG-tagged Giardia Sirtuin 2.1 only localizes to cytosol at 0 and 1.5 h of encystation (Extended data 10 e,f) which is consistent with other studies[37], suggesting Sirtuin 2.1 is not involved in the regulation of TFs in early signaling. It will be of particular interest to test whether second messengers regulate signal sensing and possibly connect to MYB2 activation, or act as a molecular switch to initiate differentiation into cysts.

Methods

Giardia growth and encystation media

Giardia intestinalis isolate WB clone C6 (ATCC catalog number 50803; American Type culture collection) were cultured in TYDK media at pH 7.1 supplemented with 10% adult bovine serum and 0.125 mg/ml bovine bile. To induce encystation, cells were cultured 48 h in pH 6.8 pre-encystation media without bile then three encystation protocols were used: (1) Uppsala encystation protocol: TYDK media at pH 7.8 supplemented with 10% adult bovine serum and 5 mg/ml bovine bile[25]; (2) Two-step protocol: TYDK media at pH 7.8 supplemented with 10% adult bovine serum, 0.25 mg/ml porcine bile and 5 mM lactic acid[38]; (3) Lipoprotein-deficient protocol: TYDK media at pH 7.8 supplemented with lipoprotein-deficient serum[39].

Plasmid construction

mNeonGreen and NanoLuc fusion

Coding sequences were PCR-amplified using *Giardia lamblia* genomic DNA as template. Primers sequences are indicated in supplemental excel file. The mNeonGreen and NanoLuc vectors were digested with the indicated restriction enzymes and the PCR amplicon was cloned in using Gibson assembly[40]. The resulting constructs were linearized with the restriction enzyme indicated in supplemental excel file before electroporation for integration into the endogenous locus[41]. Neomycin and puromycin were used for selection.

CasRX expression cassette design

EsCas13d (Catalog #108303), CasRX (Cat #109049), and PspCas13b (Cat#103862) were obtained from Addgene. Cas 13 fragments were PCR amplified, digested with restriction enzymes and

inserted into pPAC-3HA expression cassettes under the GDH promoter. The Cas13-3HA expression vectors were linearized with SwaI and electroporated into *Giardia lamblia*. To generate the CasRX expression system, CRISPRi expression vector (dCas9g1pac) [26] was used as a backbone.

Design of guide RNA

CRISPRi guide RNAs were designed based on the Dawson lab protocol[26], using the Benchling website. Cas13 guide RNA designs were based on the Sanjana lab Cas13 guide tool (https://cas13design.nygenome.org/)[42].

In vitro bioluminenscence assay

Giardia cells were iced for 15 min and centrifuged at 700 x g for 7 min at 4°C. Cells were resuspended in cold 1X HBS (HEPES-buffered saline) and serial dilution were made using MOXI Z mini Automated Cell Counter Kit (Orflo, Kenchum, ID). To measure NanoLuc luminescence, 20,000 cells were loaded into a white polystyrene, flat bottom 96-well plates (Corning Incorporated, Kennebunk, ME) then mixed with 10 µl of mixed NanoGlo luciferase assay reagent (Promega). Relative luminescence units (RLU) were detected on a pre-warmed 37°C EnVision plate reader (Perkin Elmer, Waltham, MA) for 30 min. Experiments are from three independent samples with three technical replicates. To measure CBG99 luminescence, 20,000 cells were loaded into a white polystyrene, flat bottom 96-well plates (Corning Incorporated, Kennebunk, ME) then mixed with 50 µl of D-luciferin. Relative luminescence units (RLU) was detected on a pre-warmed 37°C EnVision plate reader (Perkin Elmer, Waltham, MA) for 30 min.

Protein blotting

Giardia parasites were iced for 30 min then centrifuged at 700 x g for 7 min and washed twice in 1X HBS supplemented with HALT protease inhibitor (Pierce) and phenylmethylsulfonyl fluoride (PMSF). The cells were resuspended in 300 µl of lysis buffer (50 mM Tris-HCl pH 7.5, 150 mM NaCl, 7.5% glycerol, 0.25 mM $CaCl_2$, 0.25 mM ATP, 0.5 mM Dithiotheitol, 0.5 mM PMSF (Phenylmethylsulfonyl flroride), 0.1% Trition X-100 and Halt protease inhibitors (Pierce)). After centrifuged at 700 x g for 7 min, the supernatant was mixed with 2X sample buffer (2% SDS-62.5 mM Tris-HCl pH 6.8) and boiled at 98°C for 5 min. Protein samples were separated using sodium dodecyl sulfate (SDS) polyacriamide gel electrophoresis. Protein transfer was performed using an Immobilon-FL polyvinylidene difluoride membrane (Millipore). To detect tubulin, a mouse monoclonal anti-acetylated tubulin clone 6-11B-1 antibody (IgG2b; product T 6793; Sigma-Aldrich) were used at 1:2,500 and secondary anti-mouse isotype-specific antibody conjugated with Alexa 488 (anti-IgG2b) were used at 1:2,500. To detect CWP1, Alexa 647-conjugated anti-CWP1 antibody (Waterborne, New Orleans, LA) was used at 1:2,000. Multiplex immunoblots were imaged using a Chemidoc MP system (Bio-Rad).

Immunofluorescence

Gairdia parasites were iced for 30 min and pelleted at 700 x g for 7 min. The pellet was fixed in PME buffer (100 mM Piperazine-N,N'-bis (ethanesulfonic acid) (PIPES) pH 7.0, 5 mM EGTA, 10 mM $MgSO_4$ supplemented with 1% paraformaldehyde (PFA) (Electron Microscopy Sciences, Hatfield, PA), 100 µM 3-maleimidobenzoic acid N-hydroxysuccinimide ester (Sigma-Aldrich), 100 µM ethylene glycol bis (succinimidyl succinate) (Pierce), and 0.025% Triton X-100) for 30 min at 37°C. Fixed cells were attached on polylysine coated coverslips. Cells were washed once in PME and permeabilized with 0.1% Triton X-100 in PME for 10 min. After two quick washes with PME, blocking was performed in PME supplemented with 1% bovine serum albumin, 0.1% NaN_3, 100 mM lysine, 0.5% cold water fish skin gelatin (Sigma-Aldrich). Next, 1:200 diluted Alexa 647-conjugated anti-CWP1 antibody (Waterborne, New Orleans, LA) was added to incubate for 1 h. Cells were washed three times in PME plus 0.05% Triton X-100. Coverslips were mounted with ProLong Gold antifade plus 4',6-diamidino-2-phenylinodole (DAPI; Molecular Probes). Images were acquired on a DeltaVision Elite microscope using a 60X, 1.4-numerical apeture objective with a PCO Edge sCMOS camera, and images were deconvolved using SoftWorx (API, Issaquah, WA).

Imaging and image analysis

Analyses of CWP1-stained vesicle size and number were performed with Imaris software (Bitplane, version 8.1). ImageJ was used to process all images and figures were assembled using Adobe Illustrator.

Cyst count and cyst viability staining

To collect water-resistant *Giardia* cysts, confluent *Giardia* trophozoites were incubated in encystation media supplemented with 10 g/L ovine bovine bile and calcium lactate. To determine cyst number and viability, 48 h encysted *Giardia* cells were centrifuged at 700 x g for 7 min and the pellets were washed 10 times in deionized water, then stored in distill water overnight at 4°C. Next day, cysts were counted with a hemocytometer. For viability determination cysts were stained with fluorescein diacetate (FDA) and propidium iodide (PI) and imaged using a DeltaVision Elite microscope using a 40X, 1.4-numerical apeture objective with a PCO Edge sCMOS camera, and images were deconvolved using SoftWorx (API, Issaquah, WA).

Flow cytometry assay

Flow cytometry analyses were performed after fixation with 0.25% PFA at 4°C for 15 min. 1 µM DRAQ5 fluorescent probes (Thermo Scientific Cat# 62251) was used to stain DNA. 10,000 cells per sample were analyzed using a FACS Canto II Flow Cytometer. Data were analyzed using FlowJo.

Acknowledgements

We thank Kelli Hvorecny, Melissa Steele-Ogus, and colleagues at UW Biology for discussions and comments on the manuscripts. We thank Keyi Wang, as well as Xiaoping Wu at the UW Pathology flow cytometry facility for technical assistance. We thank Photini Sinnis, Kirk Deitsch, and Patricia Johnson for inviting us to participate at the 40th-Biology of Parasitism (BoP) course and all of the help from BoP students to initiate this project. We thank Professor Scott Dawson for gifting the CRISPRi plasmid. Research was funded by University of Washington Bridge Funding and NIH R21 AI159035 to A.R.P.

1 Schaap, P. & Schilde, C. Encystation: the most prevalent and underinvestigated differentiation pathway of eukaryotes. *Microbiology (Reading, England)* **164**, 727-739, doi:10.1099/mic.0.000653 (2018).

2 Kumar, R. & Lloyd, D. Recent advances in the treatment of Acanthamoeba keratitis. *Clinical infectious diseases : an official publication of the Infectious Diseases Society of America* **35**, 434-441, doi:10.1086/341487 (2002).

3 Fakhri, Y. *et al.* The risk factors for intestinal Giardia spp infection: Global systematic review and meta-analysis and meta-regression. *Acta tropica*, 105968, doi:10.1016/j.actatropica.2021.105968 (2021).

4 Waldram, A., Vivancos, R., Hartley, C. & Lamden, K. Prevalence of Giardia infection in households of Giardia cases and risk factors for household transmission. *BMC infectious diseases* **17**, 486, doi:10.1186/s12879-017-2586-3 (2017).

5 Wright, S. G. Protozoan infections of the gastrointestinal tract. *Infectious disease clinics of North America* **26**, 323-339, doi:10.1016/j.idc.2012.03.009 (2012).

6 Argüello-Garciá, R., Bazán-Tejeda, M. L. & Ortega-Pierres, G. Encystation commitment in Giardia duodenalis: a long and winding road. *Parasite (Paris, France)* **16**, 247-258, doi:10.1051/parasite/2009164247 (2009).

7 Lauwaet, T., Davids, B. J., Reiner, D. S. & Gillin, F. D. Encystation of Giardia lamblia: a model for other parasites. *Current opinion in microbiology* **10**, 554-559, doi:10.1016/j.mib.2007.09.011 (2007).

8 Faso, C. & Hehl, A. B. Membrane trafficking and organelle biogenesis in Giardia lamblia: use it or lose it. *Int J Parasitol* **41**, 471-480, doi:10.1016/j.ijpara.2010.12.014 (2011).

9 Bernander, R., Palm, J. E. & Svard, S. G. Genome ploidy in different stages of the Giardia lamblia life cycle. *Cell Microbiol* **3**, 55-62 (2001).

10 Byers, T. J., Kim, B. G., King, L. E. & Hugo, E. R. Molecular aspects of the cell cycle and encystment of Acanthamoeba. *Reviews of infectious diseases* **13 Suppl 5**, S373-384, doi:10.1093/clind/13.supplement_5.s373 (1991).

11 Eichinger, D. Encystation of entamoeba parasites. *BioEssays : news and reviews in molecular, cellular and developmental biology* **19**, 633-639, doi:10.1002/bies.950190714 (1997).

12 Svärd, S. G., Hagblom, P. & Palm, J. E. D. Giardia lamblia — a model organism for eukaryotic cell differentiation. *FEMS Microbiology Letters* **218**, 3-7, doi:10.1111/j.1574-6968.2003.tb11490.x (2003).

13 Larson, E. D., Marsh, A. J. & Harrison, M. M. Pioneering the developmental frontier. *Molecular cell* **81**, 1640-1650, doi:10.1016/j.molcel.2021.02.020 (2021).

14 Sun, C. H., Su, L. H. & Gillin, F. D. Novel plant-GARP-like transcription factors in Giardia lamblia. *Molecular and biochemical parasitology* **146**, 45-57, doi:10.1016/j.molbiopara.2005.10.017 (2006).

15 Su, L.-H. *et al.* A Novel E2F-like Protein Involved in Transcriptional Activation of Cyst Wall Protein Genes in Giardia lamblia*. *Journal of Biological Chemistry* **286**, 34101-34120, doi:https://doi.org/10.1074/jbc.M111.280206 (2011).

16 Pan, Y. J., Cho, C. C., Kao, Y. Y. & Sun, C. H. A novel WRKY-like protein involved in transcriptional activation of cyst wall protein genes in Giardia lamblia. *The Journal of biological chemistry* **284**, 17975-17988, doi:10.1074/jbc.M109.012047 (2009).

17 Chuang, S.-F., Su, L.-H., Cho, C.-C., Pan, Y.-J. & Sun, C.-H. Functional Redundancy of Two Pax-Like Proteins in Transcriptional Activation of Cyst Wall Protein Genes in Giardia lamblia. *PLOS ONE* **7**, e30614, doi:10.1371/journal.pone.0030614 (2012).

18 Wang, Y.-T. *et al.* A novel pax-like protein involved in transcriptional activation of cyst wall protein genes in Giardia lamblia. *J Biol Chem* **285**, 32213-32226, doi:10.1074/jbc.M110.156620 (2010).

19 Wang, C. H., Su, L. H. & Sun, C. H. A novel ARID/Bright-like protein involved in transcriptional activation of cyst wall protein 1 gene in Giardia lamblia. *The Journal of biological chemistry* **282**, 8905-8914, doi:10.1074/jbc.M611170200 (2007).

20 Waldman, B. S. *et al.* Identification of a Master Regulator of Differentiation in Toxoplasma. *Cell* **180**, 359-372.e316, doi:10.1016/j.cell.2019.12.013 (2020).

21 Sun, C.-H., Palm, D., McArthur, A. G., Svärd, S. G. & Gillin, F. D. A novel Myb-related protein involved in transcriptional activation of encystation genes in Giardia lamblia. *Molecular Microbiology* **46**, 971-984, doi:https://doi.org/10.1046/j.1365-2958.2002.03233.x (2002).

22 Ehrenkaufer, G. M., Hackney, J. A. & Singh, U. A developmentally regulated Myb domain protein regulates expression of a subset of stage-specific genes in Entamoeba histolytica. *Cellular microbiology* **11**, 898-910, doi:10.1111/j.1462-5822.2009.01300.x (2009).

23 Faso, C., Bischof, S. & Hehl, A. B. The proteome landscape of Giardia lamblia encystation. *PLoS One* **8**, e83207, doi:10.1371/journal.pone.0083207 (2013).

24 Pham, J. K. *et al.* Transcriptomic Profiling of High-Density Giardia Foci Encysting in the Murine Proximal Intestine. *Frontiers in cellular and infection microbiology* **7**, doi:10.3389/fcimb.2017.00227 (2017).

25 Einarsson, E. *et al.* Coordinated Changes in Gene Expression Throughout Encystation of Giardia intestinalis. *PLOS Neglected Tropical Diseases* **10**, e0004571, doi:10.1371/journal.pntd.0004571 (2016).

26 McInally, S. G. *et al.* Robust and stable transcriptional repression in Giardia using CRISPRi. *Mol Biol Cell* **30**, 119-130, doi:10.1091/mbc.E18-09-0605 (2019).

27 Pham, J. K. *et al.* Transcriptomic Profiling of High-Density Giardia Foci Encysting in the Murine Proximal Intestine. *Frontiers in cellular and infection microbiology* **7**, 227, doi:10.3389/fcimb.2017.00227 (2017).

28 Masser, A. E., Kandasamy, G., Kaimal, J. M. & Andréasson, C. Luciferase NanoLuc as a reporter for gene expression and protein levels in Saccharomyces cerevisiae. *Yeast (Chichester, England)* **33**, 191-200, doi:10.1002/yea.3155 (2016).

29 England, C. G., Ehlerding, E. B. & Cai, W. NanoLuc: A Small Luciferase Is Brightening Up the Field of Bioluminescence. *Bioconjugate chemistry* **27**, 1175-1187, doi:10.1021/acs.bioconjchem.6b00112 (2016).

30 Konermann, S. *et al.* Transcriptome Engineering with RNA-Targeting Type VI-D CRISPR Effectors. *Cell* **173**, 665-676.e614, doi:10.1016/j.cell.2018.02.033 (2018).

31 Cox, D. B. T. *et al.* RNA editing with CRISPR-Cas13. *Science (New York, N.Y.)* **358**, 1019-1027, doi:10.1126/science.aaq0180 (2017).

32 Huang, Y.-C. *et al.* Regulation of Cyst Wall Protein Promoters by Myb2 in Giardia lamblia*. *Journal of Biological Chemistry* **283**, 31021-31029, doi:https://doi.org/10.1074/jbc.M805023200 (2008).

33 Reiner, D. S. *et al.* Synchronisation of Giardia lamblia: identification of cell cycle stage-specific genes and a differentiation restriction point. *Int J Parasitol* **38**, 935-944, doi:10.1016/j.ijpara.2007.12.005 (2008).

34 Dawson, S. C., Nohýnková, E. & Cipriano, M. in *Giardia: A Model Organism* (eds Hugo D. Luján & Staffan Svärd) 161-183 (Springer Vienna, 2011).

35 Safi, A. *et al.* The world according to GARP transcription factors. *Current opinion in plant biology* **39**, 159-167, doi:10.1016/j.pbi.2017.07.006 (2017).

36 Lagunas-Rangel, F. A., Bazán-Tejeda, M. L., García-Villa, E. & Bermúdez-Cruz, R. M. Nicotinamide induces G2 cell cycle arrest in Giardia duodenalis trophozoites and promotes changes in sirtuins transcriptional expression. *Experimental Parasitology* **209**, 107822, doi:https://doi.org/10.1016/j.exppara.2019.107822 (2020).

37 Herrera T, E. A., Contreras, L. E., Suárez, A. G., Diaz, G. J. & Ramírez, M. H. GlSir2.1 of Giardia lamblia is a NAD+-dependent cytoplasmic deacetylase. *Heliyon* **5**, e01520, doi:https://doi.org/10.1016/j.heliyon.2019.e01520 (2019).

38 Gillin, F. D., Boucher, S. E., Rossi, S. S. & Reiner, D. S. Giardia lamblia: the roles of bile, lactic acid, and pH in the completion of the life cycle in vitro. *Experimental parasitology* **69**, 164-174, doi:10.1016/0014-4894(89)90185-9 (1989).

39 Luján, H. D., Mowatt, M. R., Byrd, L. G. & Nash, T. E. Cholesterol starvation induces differentiation of the intestinal parasite Giardia lamblia. *Proceedings of the National Academy of Sciences of the United States of America* **93**, 7628-7633, doi:10.1073/pnas.93.15.7628 (1996).

40 Gibson, D. G. *et al.* Enzymatic assembly of DNA molecules up to several hundred kilobases. *Nature Methods* **6**, 343-345, doi:10.1038/nmeth.1318 (2009).

41 Gourguechon, S., Holt, L. J. & Cande, W. Z. The Giardia cell cycle progresses independently of the anaphase-promoting complex. *Journal of cell science* **126**, 2246-2255, doi:10.1242/jcs.121632 (2013).

42 Wessels, H. H. *et al.* Massively parallel Cas13 screens reveal principles for guide RNA design. *Nature biotechnology* **38**, 722-727, doi:10.1038/s41587-020-0456-9 (2020).

Figure 1 | GARP4 and MYB1 are early signaling TFs. a, Quantification of relative expression of CWP1::NLuc, CWP2::NLuc, and CWP3::NLuc after 0, 1.5, and 4 h exposure to encystation medium (Uppsala medium). Expression level from each time point has three biological replicates. Fold change is normalized by 0 h. **b**, Localizations of MYB2::mNG after 0, 1.5, and 4 h exposure to Uppsala medium. **c**, Localizations of PAX1::mNG, GARP4::mNG and MYB1::mNG after 0 and 1.5 h exposure to Uppsala medium. **d**, Relative expression of GARP4::NLuc, MYB1::NLuc, MYB2::NLuc, and GAPDH::NLuc after 0, 1.5, 4, 7h exposure to Uppsala medium. Expression level from each time point has three biological replicates. The fold change is normalized by 0 h. Bars, 10 µm.

Figure 2 | Depletion of GARP4 increases CWP1 level and cyst number. a-c, Quantification of CRISPRi-mediated knockdowns of MYB2, MYB1, and GARP4. The expression level is normalized by dCas9 control. **d-f**, Immunoblots of CWP1 and tubulin from MYB2, MYB1, and GARP4 knockdowns. **g-i**, Quantification of immunoblots of CWP1 and tubulin from MYB2, MYB1, and GARP4 knockdowns. The expression level is normalized by tubulin control. **j-l**, Quantification of cyst number of MYB2, MYB1, and GARP4 knockdowns after 48 h encystation. Cyst counts were performed by hemocytometer. All experiments are from three independent biological replicates. Data are mean ± s.d. (n=3) Student's t-test, *p<0.01, **p<0.001, ***p<0.0001, ****p<0.00001, ns= not significant.

Figure 3| GARP4 specifically regulates encysting cell number. a, Relative protein levels of MYB1::NLuc, MYB2::NLuc, and GARP4::NLuc after 0, 0.5, 1 and 2 h exposure to encystation medium (Uppsala medium). The expression level from each time point has three biological replicates. The fold change is normalized by 0 h. **b**, Relative expression of CWP1::NLuc in GARP4 knockdowns after 0, 0.5, 1 and 2 h exposure to encystation medium (Uppsala medium). The expression level from each time point has three biological replicates. The fold change is normalized by 0 h. **c**, 24 h encysting cells of dCas9-Ctrl, GARP4-gRNA247 and GARP4-gRNA362 cell lines stained with CWP1 antibody and DAPI. Bars, 100 µm.**d**, Quantification of 24 h encysting cells of dCas9-Ctrl, GARP4-gRNA247 and GARP4-gRNA362 cell lines stained with CWP1 antibody. Percentage of encysted cells is CWP1 positive cell number divided by DPAI positive cell number. Data are mean ± s.d. (n=3) Student's t-test, *p<0.01. **e**, IMARIS-assisted analysis of vesicle number of 4 h encysted cells of dCas9-Ctrl, GARP4-gRNA247 and GARP4-gRNA362 cell lines. **f**, IMARIS-assisted analysis of vesicle volume of 4 h encysting cells cells of dCas9-Ctrl, GARP4-gRNA247 and GARP4-gRNA362 cell lines. n.s.= not significant. **g,** Quantification of trophozoite number in GARP4 knockdown from daily supplement of fresh encystation medium. **h,** Quantification of cyst number in GARP4 knockdown from daily supplement of fresh encystation medium.

Figure 4| GARP4 level is only increased in G1 cells at 1.5 h encystation. a, Cell count analysis of DRAQ5-stained cells from flow cytometry at 0 and 1.5 h encystation. Red line, separation point between G1/S and G2/M phases. **b**, Quantification of G1/S and G2/M cells from 0 and 1.5 h encystation. Data are mean ± s.d. (n=3) Student's t-test, **p<0.001. **c**, GARP4-mNG fluorescence intensity of DRAQ5-stained cells. **d**, Quantification of GARP4-mNG fluorescence intensity of G1/S and G2/M cells from 0 and 1.5 h encystation. Data are mean ± s.d. (n=3) Student's t-test, ***p<0.0001. **e,** Quantification of relative expressions of MYB2 from dCas9 control and GARP4-gRNA362 cell lines. ****p<0.00001. **f,** Quantification of relative expressions of MYB2 from tetracycline-induced GARP4-mNG overexpression cell lines. ****p<0.00001.

Extended Data Figure 1| Localizations of encystation-induced genes. Localizations of mNG-tagged E2F1(GL50803_23756), GARP3(GL50803_9154), PAX1(GL50803_32686), CCAAT-binding subunit C(GL50803_14553), CCR4-NOT subunit 7 (GL50809_8209), CCAAT-binding subunit A (GL50803_7231) and CCR-NOT subunit 7 (GL50803_10606) after 0 and 1.5 h exposure to Uppsala medium. Bars, 10 µm.

Extended Data Figure 2| E2F1, PAX1 and ARID2 are induced at 4h. Relative expression of E2F1::NLuc, PAX1::NLuc, ARID2::NLuc, and GAPDH::NLuc after 0, 1.5, 4, 7h exposure to Uppsala medium. The expression level from each time point has three biological replicates. The fold change is normalized by 0 h.

Extended Data Figure 3| Giardia CRISPRi and CasRX design. a-b, Overexpression of 3HA tagged PsCas13b, CasRX, and EsCas13d in Giardia. pGDH= promoter of glyceraldehye 3-phosphate dehydrogenease (GL50803_6877). HA=Hemagglutinin. **c**, Schematic of Giardia CRISPRi vector dCas9g1pac(ref) and CasRX vector design. pMDH= promoter of malate dehydrogenase, pac=puromycin resistance marker, 2340NLS=GL50803_2340 nuclear localization signal, SCF=gRNA scaffold sequence, DR=Direct repeat for CasRX, pU6=Giardia U6 promoter. **d**, Localizations of 3XHA tagged dCas9 and CasRX with DAPI staining in Giardia. **e,** Percentage of cells expressed dCas9 and CasRX. ****p<0.00001. Data are mean ± s.d. (n=3) Student's t-test. **f,** Growth curve of dCas9 and CasRX expressed cell lines. Blue=CasRX, Red=dCas9. Bars, 100 µm.

Extended Data Figure 4| Screen of guide RNAs with CRISPRi and CasRX systems. a, Quantification of relative protein levels of CWP1(GL50803_5638). **b,** Quantification of relative protein levels of NanoLuc. **c,** Quantification of relative protein levels of MYB1 (GL50803_5347). **d,** Quantification of relative protein levels of ARID2 (GL50803_8102). **e,** Quantification of relative protein levels of E2F1(GL50803_23756). **f,** Quantification of relative protein levels of PAX1(GL50803_32686). **g,** Quantification of relative protein levels of GARP4(GL50803_33232). **h,** Quantification of relative protein levels of MYB2(GL50803_8722). All experiments are from three independent biological replicates. Data are mean ± s.d. (n=3) Student's t-test, *p<0.01, **p<0.001, ***p<0.0001, ****p<0.00001, ns= not significant.

Extended Data Figure 5| Knockdowns of E2F1, PAX1, and ARID2 in Giardia. a-c, Quantification of CRISPRi (or CasRX)-mediated knockdowns of E2F1(GL50803_23756), PAX1(GL50803_32686), and ARID2(GL50803_8102). The expression level is normalized by dCas9 control or CasRX control. **d-f**, Immunoblots of CWP1 and tubulin from E2F1, PAX1, and ARID2 knockdowns. **g-i**, Quantification of immunoblots of CWP1 and tubulin from E2F1, PAX1, and ARID2 knockdowns. The expression level is normalized by tubulin control. All experiments are from three independent biological replicates. Data are mean ± s.d. (n=3) Student's t-test, *p<0.01, **p<0.001, ***p<0.0001, ****p<0.00001, ns= not significant.

Extended Data Figure 6| Knockdown of GARP4 and MYB1 do not alter cyst viability. a, Live and dead cysts with FDA (fluorescein diacete) and PI (prodipidium iodine) staining from 48 encysted cells of MYB1 knockdowns. **b,** Live and dead cysts with FDA (fluorescein diacete) and PI (prodipidium iodine) staining from 48 encysted cells of GARP4 knockdowns. Bars, . Data are mean ± s.d. (n=3) Student's t-test, *p<0.01, **p<0.001, ***p<0.0001, ****p<0.00001, ns= not significant. Bars, µm.

Extended Data Figure 7| Knockdown of GARP4 increases encysting cell number. a, Cell count of CWP1 antibody and DAPI stained cells at 0 h encystation in GARP4 knockdown. Bars, . **b,** Percentage of encysted cells at 0 h encystation in GARP4 knockdown. **c**, Cell count of CWP1 antibody and DAPI stained cells at 2 h encystation in GARP4 knockdown. Bars, . **d,** Percentage of encysted cells at 2 h encystation in GARP4 knockdown. **e**, Cell count of CWP1 antibody and DAPI stained cells at 4 h encystation in GARP4 knockdown. Bars, . **f,** Percentage of encysted cells at 4 h encystation in GARP4 knockdown. Data are mean ± s.d. (n=3) Student's t-test, *p<0.01, **p<0.001, ***p<0.0001, ****p<0.00001. Bars, µm.

Extended Data Figure 8| Encysted cell number at 4 h encystation in knockdowns of E2F1, PAX1 and ARID2. a, Percentage of encysted cells at 4 h encystation in E2F1 knockdown. **b**, Percentage of encysted cells at 4 h encystation in PAX1 knockdown. **c**, Percentage of encysted cells at 4 h encystation in ARID2 knockdown. **d**, Relative CWP2 levels in knockdowns of MYB1, GARP4 and MYB2 at 4 h encystation. Data are mean ± s.d. (n=3) Student's t-test, *p<0.01, **p<0.001, ****p<0.00001, ns= not significant.

Extended Data Figure 9| Knockdown of GARP4 does not alter growth rate and cell viability. a, Cell count of dCas9 control and GARP4 knockdowns at 1, 2, 3 days. 200,000 cells were added in each tube and cell numbers were measured with MOXI cell counter. **b**, Cell viability of dCas9 control and GARP4 knockdowns at 1, 2, 3 days. dCas9 control and GARP4 guide RNAs were transformed into pGDH-CBG99 expressed strain. CBG99 and D-luciferin reaction is ATP-dependent which reveals cell viability. 200,000 cells were added in each well and cell viability were detected with plate reader. Black, dcas9 control. Red, GARP4-gRNA362. Green, GARP4-gRNA247. **c**, Relative CWP1 levels in GARP4 knockdowns at 4 h encystation with lipoprotein-deficient medium or two step encystation medium. **d**, Relative CWP1 levels in GARP4-overexpression cell line at 4 h encystation. 20 mg/ml teteracycline were added to induce. Data are mean ± s.d. (n=3) Student's t-test, *p<0.01, **p<0.001, ****p<0.00001.

Extended Data Figure 10| G2/M cells have higher levels of CWP1 and MYB2. a, CWP1-mNG fluorescence intensity of DRAQ5-stained cells at 0 and 1.5 h encystation. **b**, MYB2-mNG fluorescence intensity of DRAQ5-stained cells at 0 and 1.5 h encystation. **c** , Relative E2F1 levels in GARP4 knockdown cell line at 4 h encystation. **d**, Relative PAX1 levels in GARP4 knockdown cell line at 4 h encystation.

Figure 1 |

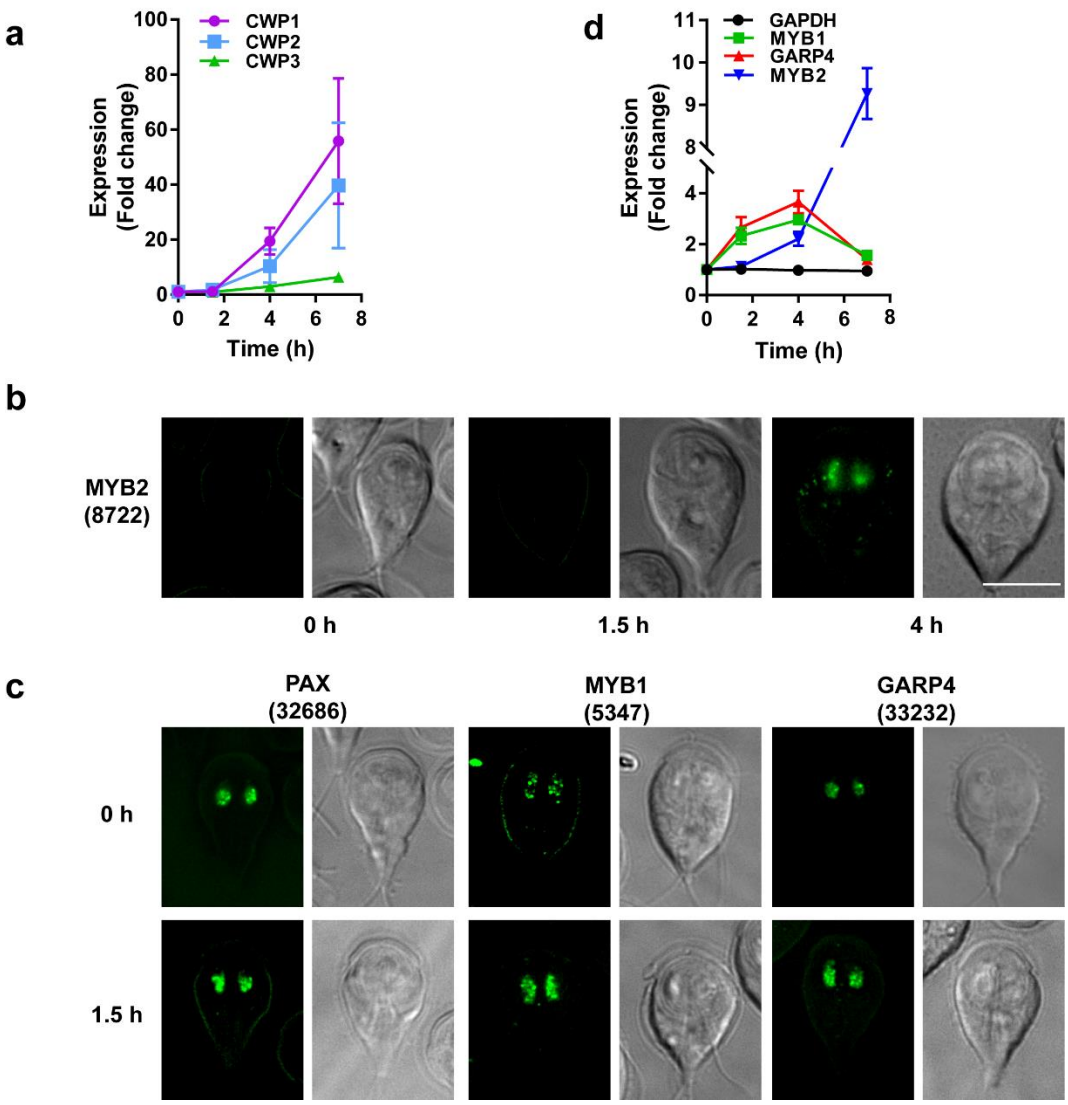

Figure 2|

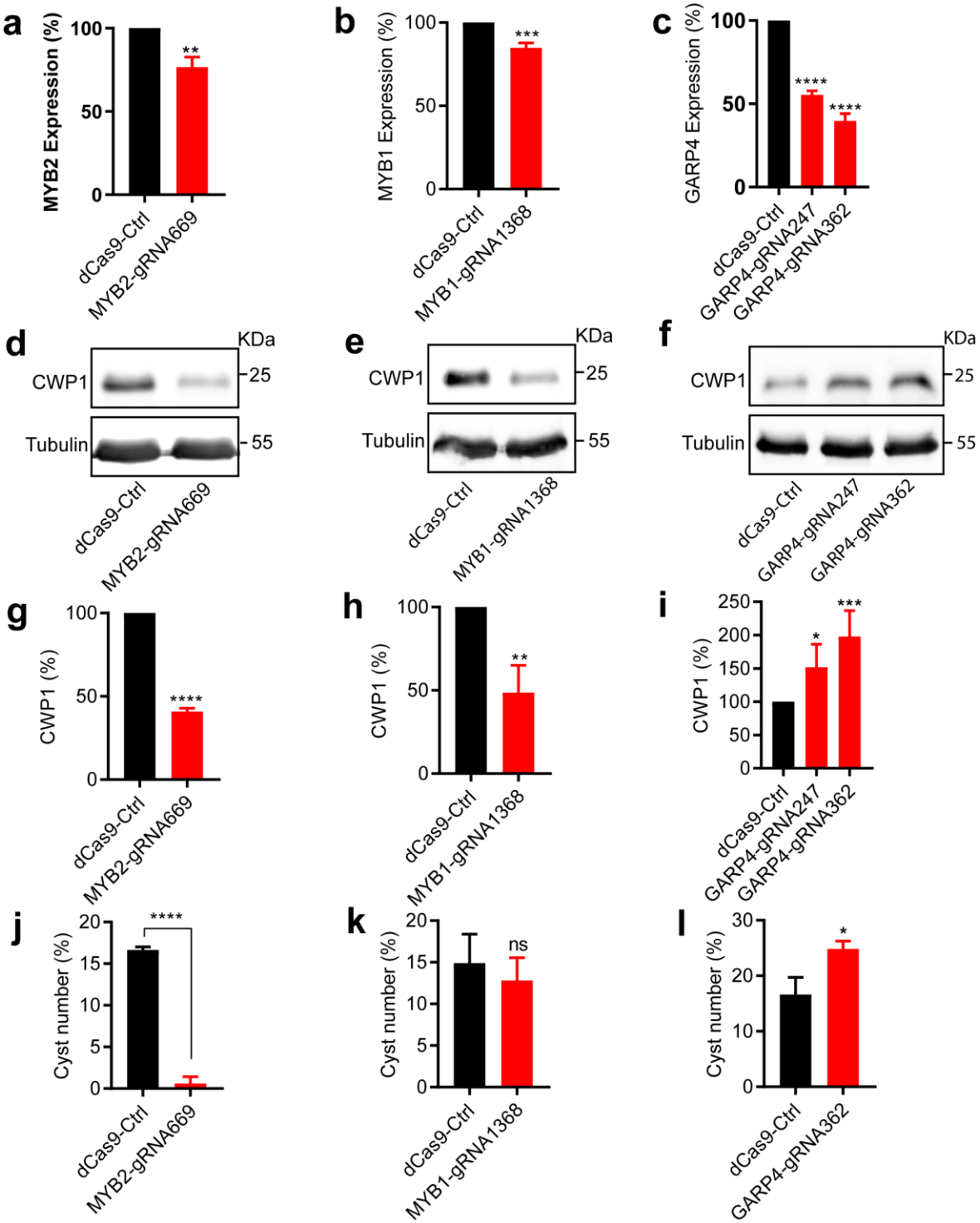

Figure 3|

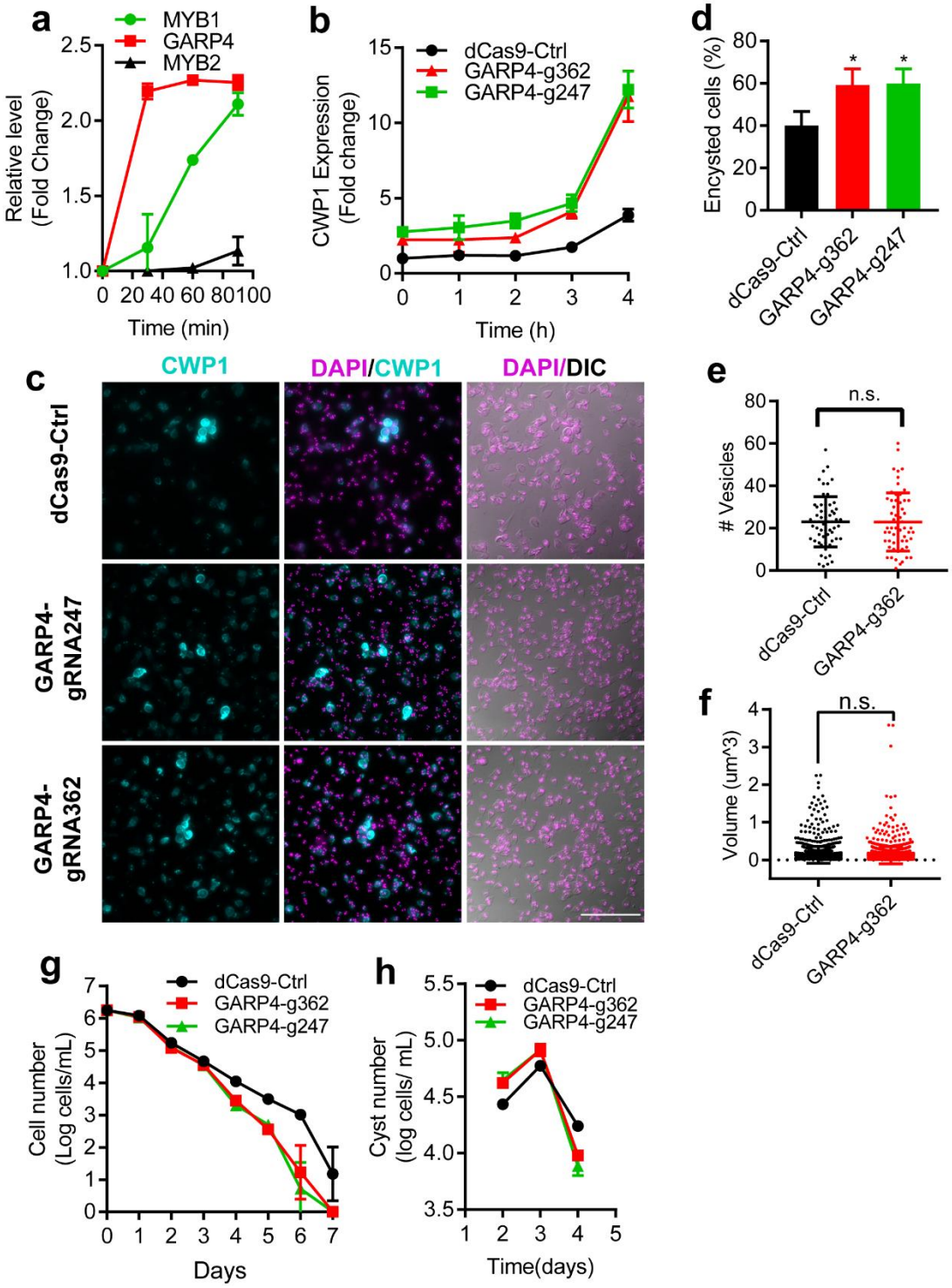

Figure 4 |